Electron Paramagnetic Resonance Spectroscopy of the Heme Domain of Inducible Nitric Oxide Synthase: Binding of Ligands at the Arginine Site Induces Changes in the Heme Ligation Geometry†

John C. Salerno,‡ Pavel Martasek,§ Linda J. Roman,§ and Bettie Sue S. Masters*,§

Rensselaer Polytechnic Institute, 15th Street, Troy, New York 12180, and The University of Texas Health Science Center at San Antonio, 7703 Floyd Curl Drive, San Antonio, Texas 78284-7760

Received March 12, 1996; Revised Manuscript Received May 6, 1996⊗

ABSTRACT: The electron paramagnetic resonance spectra of the heme domain of inducible nitric oxide synthase (iNOS) demonstrate a close relationship to the corresponding spectra of the neuronal isoform (nNOS). The binding of ligands to the iNOS arginine site perturbs the environment of the high-spin ferriheme in a highly ligand-specific manner. The iNOS forms five-coordinate, high-spin complexes with arginine analogs which are clearly related to the corresponding complexes of nNOS. Studies indicate that the binding of L-arginine, N^{ω}-hydroxy-L-arginine (NHA), and N^{ω}-methyl-L-arginine (NMA) produces various spectroscopic species closely corresponding to the equivalent complexes of nNOS, while N^{ω}-nitro-L-arginine (NNA) binding produces a state which appears intermediate in character between the nNOS NNA and arginine complexes. These spectroscopic studies have permitted the determination of ligand-specific high-spin states which reveal similarities and differences between iNOS and nNOS.

Nitric oxide synthases are complex enzymes that catalyze the conversion of L-arginine to NO and L-citrulline in a reaction that consumes 2 O_2 and $^3/_2$ NADPH per NO formed (Bromberg & Pick, 1989; Iyengar *et al.*, 1987; Marletta *et al.*, 1988; Palmer *et al.*, 1988). The constitutive endothelial and neuronal NOS isoforms are signal generators involved in the control of vascular tone (eNOS), in communication between neurons (nNOS),[1] and in other signal pathways (Garthwaite *et al.*, 1988; Palmer *et al.*, 1987). The inducible isoform (iNOS) is induced in response to an immune challenge and produces cytotoxic levels of NO (Curran *et al.*, 1989; Hauschildt *et al.*, 1990; Knowles *et al.*, 1990; McCall *et al.*, 1989). The eNOS and nNOS isoforms are controlled by Ca^{2+}/calmodulin (Abu-Soud & Stuehr, 1993), but iNOS appears to be active at all physiological Ca^{2+} levels. High levels of NO production by iNOS have been implicated in acute (toxic septicemia) and chronic (diabetes) disease processes with an autoimmune etiology (Cho *et al.*, 1992).

All NOS isoforms are modular proteins apparently formed during evolution by a series of gene fusion events resulting in the incorporation of domains binding NADPH, FAD, FMN, heme, tetrahydrobiopterin (BH_4), L-arginine, and calmodulin into a single polypeptide chain. Domains which bind FAD, FMN, and NADPH form the C-terminal ("reductase") portion of the molecule (Bredt *et al.*, 1991, 1992). Binding sites for heme, BH_4, and L-arginine are located in the "catalytic" domains (Cho *et al.*, 1995; McMillan & Masters, 1993, 1995; Nishimura *et al.*, 1995), while the calmodulin binding site links the two functional regions, which can be expressed independently (McMillan & Masters, 1995).

The binding of L-arginine or L-arginine analog inhibitors perturbs the UV−visible spectrum of the heme, reflecting shifts in the spin state equilibrium (Frey *et al.*, 1994; McMillan & Masters, 1993). Cooperativity in the binding of BH_4 and arginine has been reported (Baek *et al.*, 1993; McMillan & Masters, 1995). Recently, we showed that ligand binding at the arginine site perturbs the electron paramagnetic resonance (epr) spectrum of high-spin ferriheme without displacement of the thiolate axial ligand and (usually) without providing a sixth heme ligand (Salerno *et al.*, 1995; J. C. Salerno, K. McMillan, and B. S. S. Masters, submitted for publization). The distortion of iron ligation geometry is highly ligand-specific, reflecting specific interactions of L-arginine and its analogs within the binding site.

Because of the importance of iNOS in the development of inflammatory diseases, and the critical role of eNOS and nNOS in the regulation of physiological processes, isoform-specific inhibitors have been actively sought. In this study, we report epr spectra from iNOS catalytic domains and describe the effects of the binding of L-arginine, the catalytic intermediate, NHA, and several inhibitors on the active site geometry. The results of these studies clearly indicate similarities and differences between the nNOS and iNOS isoforms and suggest that differences in the interactions of the isoforms with substrates and inhibitors can result in spectroscopically detectable, isoform-specific variations in the environment.

† Supported in part by NIH Grant No. HL30050 and Grant No. AQ-1192 from The Robert A. Welch Foundation to B.S.S.M.

* To whom correspondence should be addressed at the Department of Biochemistry, The University of Texas Health Science Center at San Antonio, 7703 Floyd Curl Drive, San Antonio, Texas 78284-7760. Tel: (210) 567-6627. FAX: (210) 567-6984. E-mail: masters@uthscsa.edu.

‡ Rensselaer Polytechnic Institute.

§ The University of Texas Health Center at San Antonio.

⊗ Abstract published in *Advance ACS Abstracts,* June 1, 1996.

[1] Abbreviations: iNOS, inducible nitric oxide synthase (NOS2); nNOS, neuronal nitric oxide synthase (NOS1); eNOS, endothelial nitric oxide synthase (NOS3); NHA, N^{ω}-hydroxy-L-arginine; NMA, N^{ω}-methyl-L-arginine; NNA, N^{ω}-nitro-L-arginine; epr, electron paramagnetic (spin) resonance spectroscopy; GST, glutathione-*S*-transferase; BH_4, tetrahydrobiopterin.

S0006-2960(96)00607-1 CCC: $12.00

MATERIALS AND METHODS

Construction of iNOS1-500pGEX-4T1. The clone containing mouse inducible nitric oxide synthase was a gift from Dr. Anthony Persechini (University of Rochester, NY). To make iNOS1-500pGEX-4T1, primers corresponding to the coding region covering the N-terminal region and the region just before the start of the calmodulin binding motif were used to amplify the region of interest using the original clone as a template (annealing temperature = 58 °C).

The forward primer contains the *Bcl*I restriction site:

CTAATGATCAATGGCTTGCCCCTGGAA

The reverse primer contains the *Xho*I site and stop codon:

CATACTCGAGTCACAGCTTCTCATTCTGCCAGA

The PCR product was digested by *Bcl*I/*Xho*I, gel purified, and ligated to the expression plasmid pGEX-4T1 (Smith & Johnson, 1988) from Pharmacia, previously digested by *Bam*HI and *Xho*I. The entire inserted DNA was sequenced using the automated sequencer at the Center for Advanced DNA Studies at The University of Texas Health Science Center at San Antonio, using the following primers.

5′ pGEX−4T: GGGCTGGCAAGCCACGTTTGGTG

3′ pGEX−4T: CCGGGAGCTGCATGTGTCAGAGG

MAC 6R1: GAGGGAGGCCAGTGTGTG

MAC 6F1: GAGGACCCAGAGACAAGC

MAC 6F2: CAGCACATCTGCAGACAC

Full agreement was found with the published sequence (Xie *et al.*, 1992). The iNOS1-500pGEX-4T1 plasmid was used to transform the DH5α strain of *Escherichia coli*.

Protein Expression. An overnight culture of iNOS1-500pGEX-4T1 was used to inoculate 0.5 L (in a 2.8 L Fernbach flask) of Terrific Broth supplemented with ampicillin (50 μg/mL). The culture was grown to an A_{600} of ∼0.7 at 30 °C, and δ-aminolevulinic acid (0.3 mM final) was added. One hour later, 0.3 mM IPTG (final) was used for induction. The flask was shaken at 200 rpm in the dark at 22 °C; the cells were harvested 3 h after induction and frozen at −80 °C until use.

Protein Purification. Thawed cells were suspended in phosphate-buffered saline containing antiproteases (2 μg of leupeptin/mL, 2 μg of pepstatin/mL, 100 units of aprotinin/mL, 1 mM EDTA, and 0.5 mM PMSF) and lysed by mild sonication, and the crude extract was centrifuged twice at 13 000*g* for 15 min. Subsequently, the supernatant was loaded on a glutathione-Sepharose 4B column (Pharmacia), and purification of the fusion GST-iNOS1-500 protein was performed as recommended by the manufacturer. Reduction of the glutathione concentration was achieved by serial dilution/concentration using an Amicon Centriprep 30. The quality of the protein obtained was checked by SDS−PAGE; the protein bands were visualized by staining with Coomassie Blue G-250. Protein purity was estimated to be at least 70% (Figure 1).

Sample Preparation and Spectroscopy. Samples were prepared by addition of concentrated solutions of ligand to the specimen; in all cases, the volume change caused by ligand addition was <2%. Samples [0.25 mL of 15 μM protein (heme)] in 50 mM TrisHCl, pH 7.6, 10% glycerol for epr measurements were frozen in quartz epr tubes in a 6:1 isopentane−cyclohexane mixture cooled with liquid nitrogen and held in a Dewar containing liquid nitrogen until spectra were taken later on the same day. Spectra were recorded using a Bruker 300D EPR spectrometer, outfitted with an Oxford liquid helium cryostat, in the Magnetic Resonance Spectroscopy Division of the Research Imaging Center, The University of Texas Health Science Center at San Antonio. Analyses of epr spectra were performed using standard methods as previously described (Salerno *et al.*, 1995).

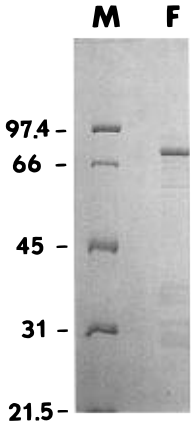

FIGURE 1: SDS−PAGE gel of GST-iNOS1-500 fusion protein using Coomassie Blue staining. 2 μg of protein was loaded in lane F; lane M was loaded with molecular mass markers.

RESULTS AND DISCUSSION

Highly purified iNOS holoenzyme has been difficult to obtain in quantities suitable for detailed spectroscopic studies. Recently, we have demonstrated that nNOS hemoprotein (consisting of the catalytic domain without the reductase domains) binds L-arginine, NHA, and certain arginine analogs, forming a series of spectrally detectable complexes which closely resemble those of the nNOS holoenzyme (K. McMillan, J. C. Salerno, M. Ikeda-Saito, and B. S. S. Masters, unpublished observations). A closely related construct containing the iNOS catalytic domain can be expressed in high yield as a glutathione-*S*-transferase (GST) fusion protein in *E. coli*, providing a system for the examination of the linkages between the L-arginine binding site and the heme site in iNOS.

Figure 2, spectrum A, shows the electron paramagnetic resonance spectrum of iNOS hemoprotein at 10 K as isolated. The g_x feature of the high-spin heme is visible at $g = 7.69$; the broad g_y feature, overlapped with the $g = 4.3$ feature of adventitious rhombic high-spin ferric iron, is present near $g \approx 4.0$. The weak g_z feature is barely visible at $g = 1.77$. The features of a low-spin ferriheme are visible at $g_z = 2.36$, $g_y = 2.26$, and $g_x = 1.92$. This represents a bisthiolate species, probably due to the binding of glutathione, which was introduced during purification. No flavin radical is visible because the reductase domains are not present in the construct.

Addition of L-arginine to the hemoprotein results in the spectrum shown in Figure 2B. The high-spin g_x feature has intensified, sharpened, and shifted to $g = 7.59$. The g_x feature is again heavily overlapped by the $g = 4.3$ species; it lies approximately at $g = 4.1$. The g_z feature is visible at

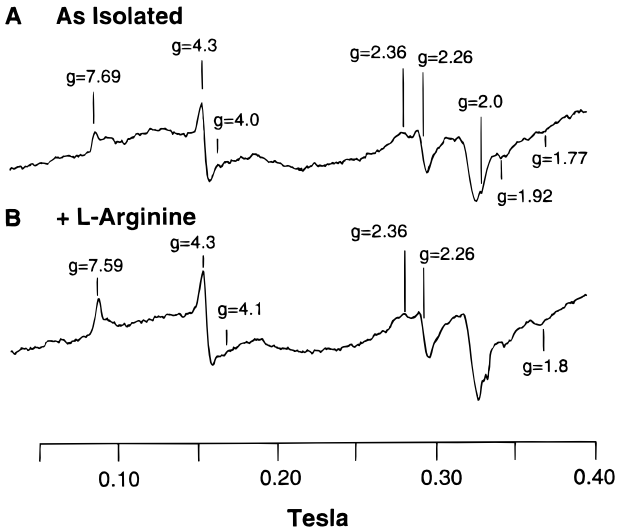

FIGURE 2: Effects of L-arginine on the electron paramagnetic resonance spectrum of iNOS ferriheme. Spectrum A: purified GST-iNOS1-500 fusion protein as isolated. Spectrum B: GST-iNOS1-500 fusion protein after addition of 100 μM L-arginine. Experimental conditions: sample temperature, 10 K; microwave power, 5 mW; modulation frequency, 100 kHz; modulation amplitude, 10 gauss; scan width, 0.4 tesla; center field, 0.21 tesla.

$g = 1.8$. In the low-spin region, the intensity at $g = 2.3$ is decreased, while intensity at $g = 2.42$ is increased, and g_y is shifted to 2.28. L-Arginine binding shifts the spin state equilibrium toward the high-spin states and also perturbs the environment of the high-spin state. Competition between arginine and glutathione appears to be responsible for the changes in the low-spin components.

In order to determine if the heme domain of iNOS retained the spectral properties of its intact form, a crude cell lysate, in which the iNOS holoenzyme was expressed, was also placed in the epr spectrometer. The data (not shown) revealed features around $g = 4.3$, which correspond to iron superoxide dismutase, while features immediately above and below $g = 2$ correspond to other cellular components. A strong peak was also observed at $g = 7.59$ which corresponds closely to the g_x feature of the iNOS heme protein−arginine complex reported, *vide infra* (Figure 2B). No other cellular components significantly interfere with this feature because only five-coordinate hemes with thiolate axial ligation are expected to contribute strong signals here. Weak features can be seen between 0.27 and 0.3 tesla, which correspond in part to low-spin components, but the high-spin g_x feature is most useful because it is free from overlap and responds to arginine analog binding.

The similarities between the iNOS g_x features are striking, implying that the iNOS heme protein described herein has a heme site with similar ligation geometry to the iNOS holoenzyme. It also appears that the iNOS holoenzyme, as expressed, is initially present primarily as the arginine complex. The data also suggest that future experiments can be performed on the cell lysates containing various constructs in order to study the effects of substrates and inhibitors subsequent to site-directed mutation since it is obvious that inhibitors can readily displace low concentrations of L-arginine. The successful preparation of a nNOS heme-GST fusion protein construct has also permitted direct comparison by epr of these constructs of both the neuronal and inducible isoforms (data not shown). The heme domains are similar to their respective holoenzymes in most respects except that they are isolated as largely low-spin species with very similar arginine- and arginine analog-binding spectra, strongly suggesting that the GST domain has little or no effect on the iNOS heme environment.

The epr spectra of high-spin ferrihemes are primarily determined by *E/D*, the ratio of the rhombic and axial zero field splitting parameters [see Salerno *et al.* (1995) and references therein]. All of the NOS high-spin complexes discussed here have *E/D* ratios indicative of five-coordinate thiolate ferrihemes. These zero field splittings can be related to ligand-induced splitting of the ferric d orbitals. The changes observed during ligand binding are thus reflections of changes in iron ligation geometry which are probably caused by the transmission of specific interactions between L-arginine analogs and the arginine-binding environment to the iron through the polypeptide. Since the first-order effect of *E/D* is to split g_x and g_y about their axial weak field value of 6, it is useful to observe these features in more detail.

Figure 3 shows epr spectra of the iNOS hemoprotein in the high-spin g_x-g_y region in order to illustrate the changes in ligation geometry of ferriheme caused by ligand binding to the arginine-binding site. Spectrum A shows the spectrum of the hemoprotein as isolated. The g_x peak of the high-spin ferriheme at $g = 7.69$ and the $g = 4.3$ rhombic iron signal are prominent; a broad high-spin heme peak at $g \approx 7.0$ can also be seen. Addition of L-arginine results in the spectrum shown in Figure 3B; the shift seen in Figure 2 is more obvious with the narrower scan. The spectral changes indicated here are highly reproducible for L-arginine and for other ligands. While it is difficult to accurately measure absolute g values in this region of the spectrum to two decimal places (because a 0.01 change in g corresponds to about 0.1 mT, and the lines are about 2 mT wide), spectra can be convincingly overlaid either on paper or digitally, and highly reproducible digital difference spectra have been obtained.

Spectrum C, Figure 3, shows the epr spectrum in the same region after addition of L-arginine and tetrahydrobiopterin. The position of g_x is the same as in the sample with L-arginine alone, but the line is even sharper and the g_y feature has been sharpened enough so that it is resolved from the $g = 4.3$ line at $g = 4.1$. When iNOS was incubated with the intermediate N^{ω}-hydroxy-L-arginine (NHA), a species with a sharp $g_x = 7.69$ feature and a well-resolved $g_y \approx 4.0$ feature was generated, as illustrated in spectrum D. A well-resolved feature at $g_z = 1.77$ could also be detected (not shown).

The inhibitors N^{ω}-methyl-L-arginine (NMA) and N^{ω}-nitro-L-arginine (NNA) bind to the arginine sites of NOS isoforms and have been reported to be partially isoform-specific in potency and mode of inhibition. These two inhibitors produced distinctive shifts in the epr spectra of the high-spin nNOS ferriheme. Also, NMA binding caused a large increase in rhombicity, producing a species with $g_x = 7.76$ and $g_y = 3.85$, while NNA binding caused a significant decrease in rhombicity, resulting in a species with $g_x = 7.26$ and $g_y = 4.43$ (J. C. Salerno, K. McMillan, and B. S. S. Masters, submitted for publication). The effects of NMA and NNA binding on iNOS hemoprotein are shown in Figure 3, spectra E and F. The NMA complex has $g_x = 7.78$ and $g_y = 3.89$, while the NNA complex has $g_x = 7.5$ and $g_y \approx 4.37$. The g_y feature is overlapped with the $g = 4.3$ signal

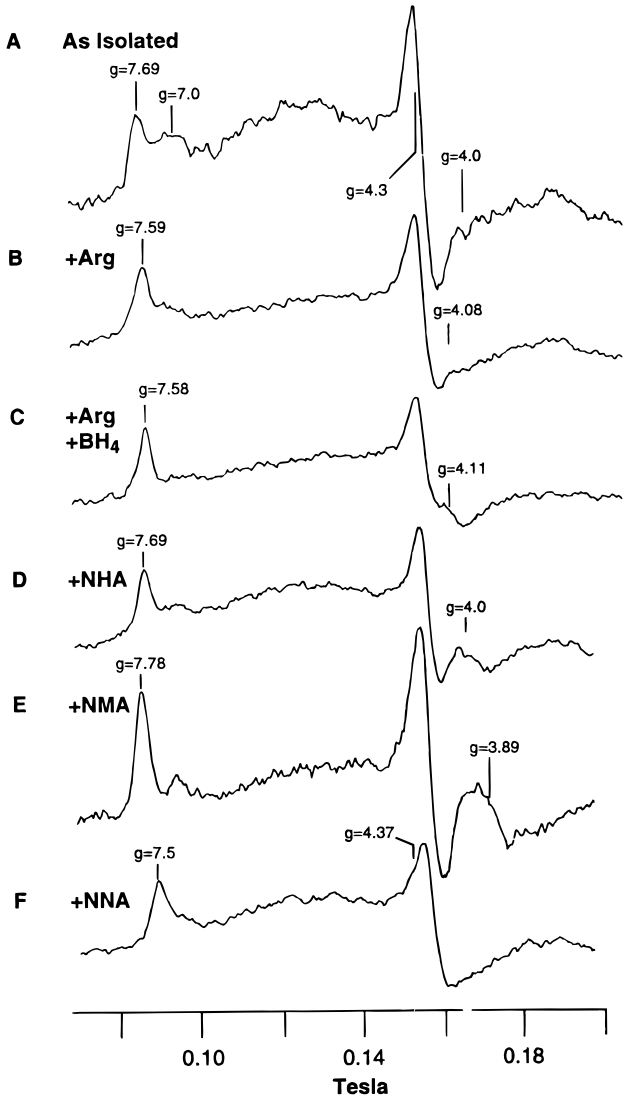

FIGURE 3: Effect of ligand binding to the arginine site on the electron paramagnetic resonance spectrum of high-spin iNOS ferriheme in the g_x-g_y region. Spectrum A: purified GST-iNOS1-500 fusion protein as isolated. Spectrum B: iNOS fusion protein after addition of 100 μM L-arginine. Spectrum C: iNOS fusion protein after addition of 100 μM L-arginine and BH_4. Spectrum D: iNOS fusion protein after addition of 100 μM NHA. Spectrum E: iNOS fusion protein after addition of 100 μM NMA. Spectrum F: iNOS fusion protein after addition of 100 μM NNA. Scan width, 0.14 tesla; center field, 0.14 tesla; other conditions as in Figure 2.

and is visible only as additional intensity on the low-field side of the line.

Figure 4 shows a series of low-spin epr spectra at 20 K to illustrate the effects of the additions on the low-spin components. Spectrum A shows the epr spectrum of the iNOS hemoprotein as isolated; features from the putative glutathione bisthiolate ferriheme are visible at $g_z = 2.36$, $g_y = 2.26$, and $g_x = 1.92$. Overlapped with these features are contributions from the native low-spin state at $g_z = 2.42$, $g_y = 2.28$, and $g_x = 1.9$. The effects of L-arginine addition are clearly visible in spectrum B; the concentration of the bisthiolate species has decreased, while the native low-spin state has increased in concentration. This suggests that iNOS hemoprotein can bind L-arginine in the low-spin state, although it is clear that L-arginine shifts the spin state equilibrium toward high-spin forms. Figure 4C shows the epr spectrum of iNOS hemoprotein in the presence of BH_4. Incubation with BH_4 leads to conversion of the remainder

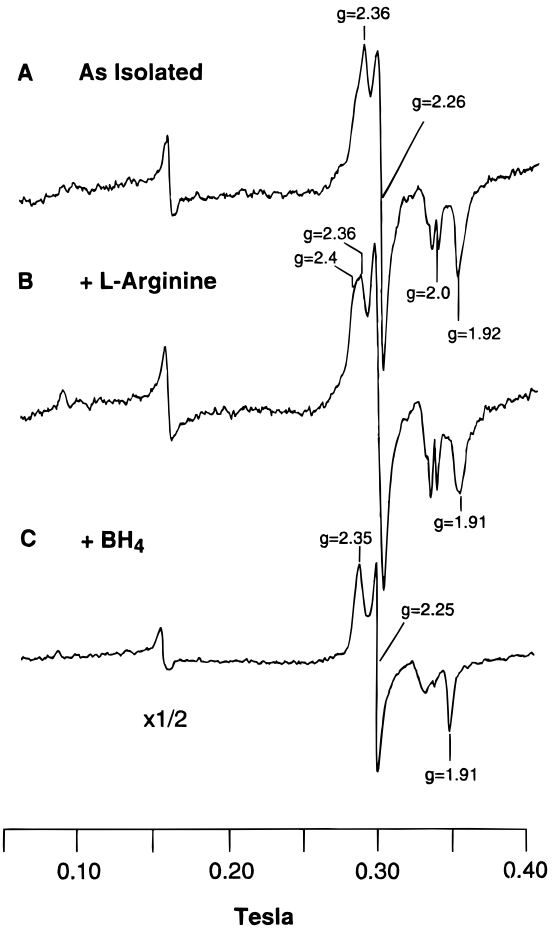

FIGURE 4: Effects on the electron paramagnetic resonance spectra of iNOS low-spin ferriheme components of the binding of L-arginine and tetrahydrobiopterin. Spectrum A: iNOS fusion protein as isolated at 20 K. Spectrum B: iNOS fusion protein after addition of L-arginine. Spectrum C: iNOS fusion protein in the presence of tetrahydrobiopterin.

of the native low-spin form of iNOS to the bisthiolate complex. Significant high-spin heme can be detected at 10 K (not shown); it appears that BH_4 favors the high-spin state in the equilibrium between native forms but that the binding of glutathione is also favored.

Recently, we showed that the binding of arginine site ligands to intact nNOS could evoke ligand-specific high-spin states which we classified in four groups (J. C. Salerno, K. McMillan, and B. S. S. Masters, submitted for publication). Group I consists of the "NMA-like" complexes, group II of "NHA-like" complexes, group III of "arginine-like" complexes, and group IV of "NNA-like" complexes. Since a similar series of states can be obtained with iNOS hemoprotein, whose heme environment closely resembles that of iNOS holoenzyme, it appears that the ligation geometry of the iNOS ferriheme is closely related to that of nNOS, but differences are present which promise insight into isoform variability in the arginine binding site.

The arginine and NHA complexes of iNOS are similar to the corresponding complexes formed by nNOS; this is consistent with the conservation of the catalytic site geometry and the shape of the substrate binding site. The NMA complex of iNOS is also quite similar to the corresponding nNOS complex. We have correlated this "group I" spectral signature with a hydrophobic substituent on a terminal amino group. The tight binding of such substituted arginines to

both nNOS and iNOS, together with the specific spectroscopic effects on the ferriheme reported here, suggest that both iNOS and nNOS have a similar pocket in contact with the arginine binding domain, possibly hydrophobic in character, which accepts the methyl group.

NNA binding to iNOS produces a less rhombic ferriheme; the shift to smaller rhombicity is in the same direction as that observed in nNOS. However, in nNOS the majority high-spin form observed had $g_x = 7.26$ and $g_y \approx 4.45$; a smaller component of intermediate rhombicity was also reported. The iNOS NNA complex appears to correspond closely to the minority high-spin NNA complex of nNOS. NNA has been reported to inactivate nNOS, but not iNOS, during preincubation (Rief & McCreedy, 1995). It appears likely that the inability of iNOS to form the majority nNOS NNA species is related to the difference in inhibitory mode.

NNA and other ligands which produce "group IV" species in nNOS present a significant steric challenge to the substrate binding site. In the case of NNA, the nitro substituent is significantly more bulky than the methyl group which produces "group I" species or the sterically similar hydrophilic groups (hydroxyl or amino) which produce "group II" species. Tight binding of NNA appears to require significant rearrangement of the substrate binding site of nNOS. The substrate binding site of iNOS may lack the flexibility to attain the configuration of the nNOS majority species, or steric differences may prevent the binding of NNA to this configuration. The possibility that the minority NNA nNOS species is a binding intermediate is attractive.

The results presented in this communication indicate that the structures directly involved in substrate binding and catalysis are highly conserved in iNOS and nNOS but that differences in the vicinity of the arginine binding site exist which give rise to limited isoform specificity. These differences are not manifested in the binding of arginine or the intermediate NHA, but inhibitors with substituents which extend the binding domain produce different states in different isoforms. This provides a powerful probe of the periphery of the substrate binding region and suggests that the spectral effects of substituted arginines can be used to map the binding site and to provide insights into the design of isoform-specific inhibitors for therapeutic and enzymological aims. Studies using a more extensive array of inhibitors and extending the work to the endothelial isoform are now in progress.

REFERENCES

Abu-Soud, H. M., & Stuehr, D. J. (1993) *Proc. Natl. Acad. Sci. U.S.A. 90*, 10769−10772.

Baek, K. J., Thiel, B. A., Lucas, S., & Steuhr, D. J., (1993) *J. Biol. Chem. 268*, 21120−21129.

Bredt, D. S., Hwang, P. M., Glatt, C. E., Lowenstein, C., Reed, R. R., & Snyder, S. H. (1991) *Nature 351*, 714−718.

Bredt, D. S., Ferris, C. D., & Snyder, S. H. (1992) *J. Biol. Chem. 267*, 10976−10981.

Bromberg, Y., & Pick, E. (1989) *Cell. Immunol. 52*, 73−83.

Cho, H. J., Xie, Q., Calaycay, J., Mumford, R. E., Swiderek, K. M., Lee, T. D., & Nathan, C. (1992) *J. Exp. Med. 176*, 599−604.

Cho, H. J., Martin, E., Xie, Q-w., Sassa, S., & Nathan, C. (1995) *Proc. Natl. Acad. Sci. U.S.A. 92*, 11514−11518.

Curran, R. D., Billiar, T. R., Stuehr, D. J., Hofmann, K., & Simmons, R. L. (1989) *J. Exp. Med. 170*, 1769−1774.

Frey, C., Narayanan, K., McMillan, K., Spack, L., Gross, S. S., Masters, B. S. S., & Griffith, O. W. (1994) *J. Biol. Chem. 269*, 26083−26091.

Garthwaite, J., Charles, S. L., & Chess-Williams, R. (1988) *Nature 336*, 385−388.

Hauschildt, S., Lucknoff, A., Mulsch, A., Kohler, J., Bessler, W., & Buse, R. (1990) *Biochem. J. 270*, 351−356.

Iyengar, R., Stuehr, D. J., & Marletta, M. A. (1987) *Proc. Natl. Acad. Sci. U.S.A. 84*, 6369−6373.

Knowles, R. G., Palacios, M., Palmer, R. M. J., & Moncada, S. (1990) *Biochem. J. 269*, 207−210.

Marletta, M. A., Yoon, P. Y., Iyengar, R., Leaf, C. D., & Wishnok, J. S. (1988) *Biochemistry 27*, 8706−8711.

McCall, T. B., Boughton-Smith, N. K., Palmer, R. M. J., Whittle, B. J. R., & Moncada, S. (1989) *Biochem. J. 262*, 293−296.

McMillan, K., & Masters, B. S. S. (1993) *Biochemistry 32*, 9875−9880.

McMillan, K., & Masters, B. S. S. (1995) *Biochemistry 34*, 3686−3693.

Nishimura, J. S., Martasek, P., McMillan, K., Salerno, J. C., Liu, Q., Gross, S. S., & Masters, B. S. S. (1995) *Biochem. Biophys. Res. Commun. 210*, 288−294.

Palmer, R. M. J., Ferrige, D. S., & Moncada, S. (1987) *Nature 327*, 524−526.

Palmer, R. M. J., Ashton, A. G., & Moncada, S. (1988) *Nature 333*, 664−666.

Rief, D. W., & McCreedy, S. A. (1995) *Arch. Biochem. Biophys. 320*, 170−176.

Salerno, J. C., Frey, C., McMillan, K., Williams, R., Masters, B. S. S., & Griffith, O. W. (1995) *J. Biol. Chem. 270*, 27423−27428.

Smith, D. B., & Johnson, K. S. (1988) *Gene 67*, 31−40.

Xie, Q., Cho, H. J., Calacay, J., Mumford, R. A., Swiderek, K. M., Lee, T. D., Ding, A., Troso, T., & Nathan, C. (1992) *Science 256*, 225−228.

BI960607L